

18 **Abstract**

19 Chemosensory systems are critical for evaluating the caloric value and potential toxicity of food
20 prior to ingestion. While animals can discriminate between 1000's of odors, much less is known
21 about the discriminative capabilities of taste systems. Fats and sugars represent calorically
22 potent and innately attractive food sources that contribute to hedonic feeding. Despite the
23 differences in nutritional value between fats and sugars, the ability of the taste system to
24 discriminate between different rewarding tastants is thought to be limited. In *Drosophila*, sweet
25 taste neurons expressing the Ionotropic Receptor 56d (*IR56d*) are required for reflexive
26 behavioral responses to the medium-chain fatty acid, hexanoic acid. Further, we have found
27 that flies can discriminate between a fatty acid and a sugar in aversive memory assays,
28 establishing a foundation to investigate the capacity of the *Drosophila* gustatory system to
29 differentiate between various appetitive tastants. Here, we tested whether flies can discriminate
30 between different classes of fatty acids using an aversive memory assay. Our results indicate
31 that flies are able to discriminate medium-chain fatty acids from both short- and long-chain fatty
32 acids, but not from other medium-chain fatty acids. Characterization of hexanoic acid-sensitive
33 *Ionotropic receptor 56d* (*Ir56d*) neurons reveals broad responsive to short-, medium-, and long-
34 chain fatty acids, suggesting selectivity is unlikely to occur through activation of distinct sensory
35 neuron populations. However, genetic deletion of *IR56d* selectively disrupts response to
36 medium chain fatty acids, but not short and long chain fatty acids. These findings reveal *Ir56d* is
37 selectively required for fatty acid taste, and discrimination of fatty acids occurs through
38 differential receptor activation within shared populations of neurons. These findings uncover a
39 capacity for the taste system to encode tastant identity within a taste category.

40 Introduction

41 Animals detect food primarily through taste and olfactory systems. Across phyla, there is
42 enormous complexity in olfactory receptors and downstream processing mechanisms that allow
43 for detection and differentiation between odorants (Keller et al., 2017; Nara, Saraiva, Ye, &
44 Buck, 2011; Parnas, Lin, Huetteroth, & Miesenböck, 2013). By contrast, taste coding is thought
45 to be simpler, with most animals possessing fewer taste receptors and a diminished ability to
46 differentiate between tastants (Freeman & Dahanukar, 2015; Scott, 2018; Yarmolinsky, Zuker, &
47 Ryba, 2009). Most early studies in different species have focused on characterization of a
48 limited number of taste modalities largely defined by human percepts (sweet, bitter, sour,
49 umami, salt), though there is growing appreciation that additional taste pathways are likely to
50 influence gustatory responses and feeding (Chaudhari & Roper, 2010; Scott, 2018). Between
51 studies of *Drosophila* and mammals, cells or receptors that are involved in sensing water,
52 carbonation, fat, electrophiles, polyamines, metal ions, and ribonucleotides have been identified,
53 suggesting a previously underappreciated complexity in the coding of tastants (Cameron, Hiroi,
54 Ngai, & Scott, 2010; Kang et al., 2010; Mishra, Thorne, Miyamoto, Jagge, & Amrein, 2018; Y. V.
55 Zhang, Ni, & Montell, 2013). Elucidating the underlying mechanisms of tastant detection can
56 provide fundamental insight into the molecular and cellular basis of tastant recognition and taste
57 processing.

58
59 In flies and mammals, tastants are sensed by dedicated gustatory receptors that are expressed
60 in gustatory receptor neurons (GRNs) or taste cells respectively. In both systems, distinct
61 subsets of taste sensory cells are activated by compounds belonging to distinct taste modalities
62 such as sweet or bitter, and convey information to discrete areas of higher order brain structures
63 (Vosshall & Stocker, 2007; Yarmolinsky et al., 2009; Yifeng Zhang et al., 2003). Given the
64 conserved logic of taste processing, flies provide a powerful system for studying sensory
65 processing and principles of taste circuit function (Freeman & Dahanukar, 2015; Scott, 2018;

66 Yarmolinsky et al., 2009). Further, a number of genes and biochemical pathways that regulate
67 feeding behavior are conserved across phyla (Vosshall & Stocker, 2007; Yarmolinsky et al.,
68 2009). Notably, the gustatory system of *Drosophila* is amenable to *in vivo* Ca²⁺ imaging and
69 electrophysiology, both of which can be coupled with robust behavioral assays that measure
70 reflexive taste responses and food consumption (Wisotsky, Medina, Freeman, & Dahanukar,
71 2011). Taste neurons are housed in gustatory sensory structures called sensilla, which are
72 located in the distal segments of the legs (tarsi), in the external and internal mouth organs
73 (proboscis and pharynx), and in the wings. Each sensillum contains dendrites of multiple
74 gustatory receptor neurons, each of which can be distinguished from the others based on its
75 responses to various categories of tastants. Two main classes of non-overlapping gustatory
76 neurons that have been identified are sweet-sensing and bitter-sensing neurons. Sweet-sensing
77 GRNs promote feeding, whereas bitter-sensing GRNs act to deter (Marella et al., 2006; Thorne,
78 Chromey, Bray, & Amrein, 2004). Both sweet and bitter GRNs express subsets of 68 G-protein-
79 coupled gustatory receptors (GRs) (Clyne, Warr, & Carlson, 2000; Scott et al., 2001). In
80 addition, the *Drosophila* genome encodes 66 glutamate-like Ionotropic Receptors (IRs), a
81 recently identified family of receptors implicated in taste, olfaction, and temperature sensation
82 (Benton, Vannice, Gomez-Diaz, & Vosshall, 2009; Rytz, Croset, & Benton, 2013). GRNs
83 predominantly project to the subesophageal zone (SEZ), the primary taste center, but the higher
84 order circuitry downstream of the SEZ contributing to taste processing is poorly understood
85 (Flood et al., 2013; Marella, Mann, & Scott, 2012; Pool et al., 2014; Wang, Singhvi, Kong, &
86 Scott, 2004). Determining how tastants activate GRNs that convey information to the SEZ, and
87 how these signals are transmitted to higher order brain centers, is central to understanding the
88 neural basis for taste and feeding.

89

90 In *Drosophila*, GRNs in the labellum and tarsi detect hexanoic acid (Pavel Masek & Keene,
91 2013). Mutation of Ionotropic receptor 56d (*IR56d*) disrupts hexanoic acid taste, implicating

92 *IR56d* as a fatty acid receptor, or as part of a complex involved in fatty acid taste (Ahn, Chen, &
93 Amrein, 2017; Sánchez-Alcañiz et al., 2018). *IR56d* is co-expressed with Gr64f (Ahn et al.,
94 2017; Tauber et al., 2017), which broadly labels sweet GRNs (Dahanukar, Lei, Kwon, &
95 Carlson, 2007; Jiao, Moon, Wang, Ren, & Montell, 2008; Slone, Daniels, & Amrein, 2007).
96 *IR56d*-expressing GRNs are responsive to both sugars and fatty acids, suggesting that these
97 neurons may respond to diverse appetitive substances including multiple classes of fatty acids
98 (Tauber et al., 2017). Notably, overlapping populations of sweet GRNs that are responsive to
99 different appetitive modalities and confer feeding behavior.

100

101 Is it possible that flies are capable of differentiating between tastants of the same modality, or is
102 discrimination within a modality exclusively dependent on concentration? Taste discrimination
103 can be assayed by training flies to pair a negative stimulus with a tastant, and determining
104 whether the acquired aversion generalizes to another tastant (Keene & Masek, 2012; Pavel
105 Masek & Scott, 2010). A previous study employing such experiments found that flies are unable
106 to discriminate between different sugars (Pavel Masek & Scott, 2010). Conversely, we reported
107 that flies can discriminate between sucrose (sugar) and hexanoic acid (fatty acid), revealing an
108 ability to discriminate between appetitive stimuli of different modalities (Tauber et al., 2017).
109 Here, we find that flies are capable of discriminating between different classes of fatty acids,
110 despite broad tuning of fatty-acid sensitive neurons to short, medium and long chain FAs.

111

112 **Results**

113 Sugars and medium chain fatty acids are sensed by an overlapping population of gustatory
114 neurons, and flies can discriminate between these attractive tastants (Ahn et al., 2017; Tauber
115 et al., 2017). To test whether flies are capable of discriminating within a single modality, we
116 measured the ability of flies to discriminate between different types of fatty acids. We have used
117 an appetitive taste memory assay in which an appetitive tastant is paired with bitter quinine,

118 resulting in an associative memory that inhibits responses to the appetitive tastant (Pavel
119 Masek, Worden, Aso, Rubin, & Keene, 2015). A modified version of this assay, in which training
120 with one tastant is followed by testing with another, allows us to determine whether flies can
121 discriminate between these tastants (Fig 1A). We first sought to determine whether flies are
122 capable of differentiating between short (3C-5C), medium (6C-8C) and long (>9C) FAs. We
123 found that flies that were trained with pairing of quinine and hexanoic acid (6C) exhibited PER to
124 subsequent application of 5C fatty acids (Fig 1B). Thus, aversive memory to 5C was not formed
125 by training with 6C, suggesting that flies can discriminate between these short- and medium-
126 chain fatty acids. Similarly, flies trained with 6C did not generalize aversive memory to 9C,
127 consistent with the idea that flies can also discriminate between medium- and long-chain fatty
128 acids (Fig 1C). To rule out the possibility that flies are unable to form aversive taste memories to
129 short- and long-chain fatty acids, we trained with 5C and found robust aversive taste memory,
130 which did not generalize to 9C (Fig 1D). Together, these results suggest that flies are capable of
131 distinguishing between short, medium and long-chain classes of fatty acids.

132
133 To determine whether flies can discriminate between compounds within a single class of fatty
134 acid, we tested the ability of flies to differentiate between different medium-chain fatty acids. We
135 trained flies to associate 6C with quinine, while the medium-chain fatty acids 7C or 8C were not
136 reinforced. In both cases, flies formed aversive memories to 6C, and this generalized to 7C and
137 8C, suggesting that flies cannot discriminate between different medium chain fatty acids (Fig
138 1E,F). To fortify these findings, we trained flies to 7C and measured the response to 8C. Again,
139 flies formed aversive memory to 7C that was generalized to 8C (Fig 1G). Our findings reveal
140 that flies cannot discriminate between different medium chain fatty acids, although they are able
141 to discriminate medium-chain fatty acids from short- or long-chain fatty acids.

142

143 The short, medium, and long-chain fatty acids that we tested have distinctly different smells
144 (Hallem & Carlson, 2006), raising the possibility that flies can discriminate between these
145 compounds using a combination of olfactory and gustatory information. To exclude the effects of
146 olfactory input, we surgically ablated the antennae, the maxillary palps, or both structures, and
147 measured the ability of flies to discriminate between a representative tastant from each short-,
148 medium-, or long-chain fatty acid (Fig 2A). All test groups were able to distinguish between
149 sucrose and hexanoic acid, confirming that the ablation itself does not generally impact taste or
150 memory formation (Fig 2B). Further, flies trained to a medium-chain fatty acid (6C) did not
151 generalize aversion to short- (5C) or long-chain (9C) fatty acids, regardless of the absence of
152 one or both olfactory organs (Fig 2C,D). Taken together, our findings reveal an ability of the
153 taste system to encode the identity of different classes of fatty acids.

154
155 The finding that flies cannot discriminate between medium chain fatty acids raises the possibility
156 that *IR56d* is required for the taste of medium-chain fatty acids, but not short and long-chain
157 fatty acids. To determine whether *IR56d*-expressing GRNs mediate taste perception to other
158 classes of fatty acids, we silenced *IR56d*-expressing neurons using the synaptobrevin cleavage
159 peptide tetanus toxin light chain (TNT) (Sweeney, Brodie, Keane, Niemann, & Kane, 1995) and
160 measured proboscis extension response (PER) to multiple classes of fatty acids, including
161 short-, medium-, and long-chain fatty acids (Figure 3A). To control for any non-specific effects of
162 TNT, we compared PER in flies with silenced *IR56d* GRNs (*IR56d*-GAL4>UAS-TNT) to flies
163 expressing the inactive variant of TNT in *IR56d*-expressing GRNs (*IR56d*-GAL4>UAS-impTNT).
164 Consistent with previous findings (Tauber et al., 2017), we observed no effect of silencing
165 *IR56d*-expressing neurons on PER to sucrose (Figure 3B). Next, we measured PER to a panel
166 of saturated FAs ranging from 4C (butanoic acid) to 10C (decanoic acid) in length (Figure 3C).
167 Control flies exhibited a robust PER to all seven fatty acids, revealing that at least at a 1%
168 concentration, many diverse classes of fatty acids can trigger this behavioral response. To

169 determine whether *IR56d* is generally required for detection of fatty acids, or selectively required
170 for sensing hexanoic acid, we next measured PER in flies with *IR56d*-expressing neurons
171 silenced. Silencing *IR56d*-expressing neurons significantly reduced PER to the three medium
172 chain fatty acids (6C, 7C, and 8C). Conversely, there was no difference in PER between control
173 and *IR56d*-silenced flies in response to short chain (4C and 5C) and long-chain (9C and 10C)
174 fatty acids. Therefore, *IR56d*-expressing neurons are required for medium-chain fatty acid taste
175 perception, but are dispensable for responses to both short- and long-chain fatty acids.

176
177 To directly assess whether the *IR56d* receptor mediates responses to medium chain fatty acids,
178 we used the CRISPR/Cas9 system to generate an *IR56d* allele in which a GAL4 element is
179 inserted into the *IR56d* locus (*IR56d*^{GAL4}; Figure 4A), thereby allowing expression of UAS-
180 transgenes under the control of the *IR56d* promoter. To confirm that the GAL4 knock-in element
181 is indeed expressed in *IR56d* neurons, we generated flies carrying both UAS-mCD8:GFP and
182 the *IR56d*^{GAL4} allele (*IR56d*^{GAL4}>UAS-mCD8:GFP) and mapped the expression of GFP.
183 Consistent with previous findings, we found GFP expression in labellar neurons that projected
184 axons to both the taste peg and sweet taste regions of the SEZ (Figure 4B-E; (Koh et al., 2014;
185 Tauber et al., 2017). In agreement with previous findings from genetic silencing of *IR56d*-
186 expressing neurons, PER to sucrose did not differ between *IR56d*^{GAL4} and control flies (Figure
187 4F), suggesting that *IR56d*^{GAL4} is dispensable for response to sucrose. To examine the role of
188 *IR56d* in fatty acid taste, we measured PER to fatty acids ranging from 4C to 10C in length
189 (Figure 4G). Consistent with the results of *IR56d*-silenced flies, PER to medium chain fatty acids
190 was disrupted in *IR56d*^{GAL4} flies (6C-8C), whereas PER to short- (4C and 5C) and long-chain
191 fatty acids (9C and 10C) was not affected. Flies that were heterozygous for the *IR56d* deletion
192 (*IR56d*^{GAL4/+}) exhibited similar responses to those of control flies for all tastants measured. The
193 observed decrease in PER to medium chain fatty acids was rescued by transgenic expression
194 of *IR56d* in the *IR56d*^{GAL4} mutant background (*IR56d*^{GAL4}; UAS-*IR56d*/+), confirming that the

195 behavioral deficit of *IR56d*^{GAL4} flies is in fact due to loss of *IR56d* function. Therefore, *IR56d*
196 appears to be selectively required for taste sensing of medium-chain fatty acids.

197

198 In previous work we found that *IR56d*-expressing neurons are activated by both sucrose and
199 hexanoic acid (Tauber et al., 2017). To determine whether other classes of fatty acids can also
200 activate these neurons, and if so, whether their activity is dependent on *IR56d*, we measured
201 Ca²⁺ responses to a panel of tastants. We expressed the Ca²⁺ sensor GCaMP6.0 under the
202 control of *IR56d*^{GAL4} and measured tastant-evoked activity (Figure 5A-D). In flies heterozygous
203 for *IR56d*^{GAL4}, the labeled neurons were activated by sucrose and all fatty acids tested, which
204 ranged from 4C-10C (Figure 5E). Thus, *IR56d* neurons respond to diverse appetitive stimuli.
205 Flies with a deletion of *IR56d*^{GAL4} (*IR56d*^{GAL4}; *UAS-GCaMP6.0*) lacked responses exclusively to
206 medium chain fatty acids (6C-8C), while responses to short- (4C and 5C) and long-chain fatty
207 acids (9C and 10C) remained intact (Figure 5F). Consistent with the rescue of behavioral
208 defects, inclusion of an *IR56d* rescue transgene (*IR56d*^{GAL4}; *UAS-GCaMP6.0/UAS-IR56d*)
209 restored the physiological response to medium chain fatty acids (Figure 5G). Quantification of
210 the responses to all tastants confirmed that Ca²⁺ responses to 6C-8C fatty acids are disrupted in
211 *IR56d*^{GAL4} flies, and restored to levels observed in control flies by expression of *IR56d* (Figure
212 5H). Overall, these results demonstrate that at both behavioral and physiological levels,
213 *IR56d*^{GAL4} is required for taste responses to medium chain fatty acids. Therefore, these findings
214 support the notion that medium chain fatty acids are detected through a shared sensory
215 channel, allowing flies to distinguish medium chain from short or long-chain, but not between
216 different medium-chain fatty acids.

217

218 Discussion

219 Receptors for sweet and bitter taste have been well defined in both flies and mammals
220 (Carleton, Accolla, & Simon, 2010; Hallem, Dahanukar, & Carlson, 2006; Scott, 2018), but less

221 is known about detection of fats. Previous studies identified *IR56d* as a receptor for hexanoic
222 acid and carbonation (Ahn et al., 2017; Sánchez-Alcañiz et al., 2018). Our findings suggest that
223 *IR56d* is selectively involved in responses to medium-chain fatty acids, including 6C, 7C, and
224 8C fatty acids, and dispensable for responses to shorter and longer-chain fatty acids. Such
225 receptor specificity for different classes of fatty acids based on chain length has not been
226 documented in other systems. In flies, both sugars and fatty acids activate neurons that co-
227 express the receptors *Gr64f* and *IR56d*. The finding that short- and long-chain fatty acids also
228 activate *IR56d*-expressing neurons posits that additional fatty acid receptors are present in
229 these neurons. Previously, we found that deletion of PLC signaling selectively impairs hexanoic
230 acid response while leaving sweet taste intact, raising the possibility that activation of distinct
231 intracellular signaling pathways could serve as a mechanism for discrimination of sucrose and
232 hexanoic acid (Pavel Masek & Keene, 2013; Tauber et al., 2017). Examining whether or not
233 short- and long-chain fatty acids also signal through phospholipase C may provide insight into
234 whether signaling mechanisms are shared between different fatty acid receptors expressed in
235 *IR56d* neurons.

236
237 Our aversive taste memory assay confirmed previous findings that flies can discriminate
238 between sugars and fatty acids (Tauber et al., 2017), and led to the surprising observation that
239 flies can distinguish between different classes of fatty acids. This contrasts with the results of a
240 previous study that applied a similar assay and found that flies were unable to discriminate
241 between different sugars or bitter compounds (Kirkhart & Scott, 2015). One possibility is that
242 this is due to differences in fatty acid detection, which is dependent on IRs, and sweet and bitter
243 tastant detection, which relies on GRs (Chen & Dahanukar, 2020). These results suggest the
244 ability of the *Drosophila* the taste system to discriminate may be more like the olfactory system
245 than previously appreciated. Flies are able to distinguish between many different odorants, likely
246 due to the complexity of olfactory coding at the level of the receptor as well as in the antennal

247 lobe (Amin & Lin, 2019; Cognigni, Felsenberg, & Waddell, 2018; Guven-Ozkan & Davis, 2014).
248 However, flies can also discriminate between odorants sensed by a single olfactory receptor,
249 suggesting that temporal coding also plays a role in discrimination (DasGupta & Waddell, 2008).
250 It is possible that similar mechanisms underlie discrimination between different classes of fatty
251 acid tastants.

252
253 The *Drosophila* genome encodes 66 Ionotropic Receptors (IRs), which comprise a recently
254 identified family of receptors implicated in taste, olfaction, and temperature sensation (Benton et
255 al., 2009; Rytz et al., 2013). Ionotropic receptors are involved in the detection of many different
256 tastants, and function as heteromers that confer sensory specificity (Rytz et al., 2013; van
257 Giesen & Garrity, 2017). While *IR56d* expression is restricted to a subset of sweet taste
258 neurons, it likely functions in a complex with *IR25a* and *IR76b*, all three of which are required
259 fatty acid taste (Ahn et al., 2017; Sánchez-Alcañiz et al., 2018). Other tastants whose responses
260 are mediated by IR receptors are also likely to be detected by IR complexes. For example, roles
261 for *IR25a*, *IR62a* and *IR76b* have been described for Ca²⁺ taste (Thakur, Kim, Poudel, Montell,
262 & Lee, 2017). The broad degree of co-expression of IRs in the brain and periphery can provide
263 candidates for those involved in detecting short- and long-chain fatty acids.

264
265 The identification of taste discrimination between different classes of fatty acids provides the
266 opportunity to identify how different tastants are encoded in the brain, and how these circuits are
267 modified with experience. Although projections of primary taste neurons to the SEZ have been
268 mapped in some detail, little is known about connectivity with downstream neurons and whether
269 sensory neurons activated by different appetitive tastants can activate different downstream
270 circuits. Recent studies have identified a number of interneurons that modify feeding, including
271 IN1, a cholinergic interneuron activated by sucrose (Yapici, Cohn, Schusterreiter, Ruta, &
272 Vosshall, 2016), E564 neurons that inhibit feeding (Mann, Gordon, & Scott, 2013), and *Fdg*

273 neurons that are required for sucrose-induced feeding (Flood et al., 2013). Future work can
274 investigate whether these, and other downstream neurons, are shared for fatty acid taste.
275 Previous studies have found that incoming sensory information is selectively modulated within
276 the antennal lobe in accordance with feeding state (Chu, Chui, Mann, & Gordon, 2014; LeDue
277 et al., 2016). It will be interesting to determine if similar modulation promotes differentiation of
278 sugars and fatty acids, which are sensed by shared gustatory neurons. Large-scale brain
279 imaging has now been applied in flies to measure responsiveness to different tastants (Harris,
280 Kallman, Mullaney, & Scott, 2015), and a comparison of brain activity patterns elicited by
281 different classes of fatty acids may provide insight into differences in their sensory input and
282 processing.

283

284 All experiments in this study tested flies under starved conditions, which is necessary to elicit
285 the PER that is used as a behavioral readout of taste acceptance. However, responses to many
286 tastants and odorants are altered in accordance with feeding state (LeDue et al., 2016; Root et
287 al., 2008). For example, the taste of acetic acid is aversive to fed flies but attractive to starved
288 flies, revealing a hunger-dependent switch (Devineni, Sun, Zhukovskaya, & Axel, 2019).
289 Similarly, hexanoic acid activates both sweet and bitter sensing taste neurons, and the
290 activation of bitter taste neurons is dependent on different receptors from those involved in the
291 appetitive response (Ahn et al., 2017). Further, hunger enhances activity in sweet taste circuits,
292 and suppresses that of bitter taste circuits, providing a mechanism for complex state-dependent
293 modulation of response to tastants that activate both appetitive and deterrent neurons (Inagaki,
294 Panse, & Anderson, 2014; LeDue et al., 2016).

295

296 The neural circuits that are required for aversive taste memory have been well defined for
297 sugar, yet little is known about how fatty acid taste is conditioned. The pairing of sugar with
298 bitter quinine results in aversive memory to sugar. Optogenetic activation of sweet taste

299 neurons, which are activated by both sugar and fatty acids, in combination with quinine
300 presentation is sufficient to induce sugar avoidance, suggesting that aversive taste memory
301 does not depend on post-ingestive feedback (Keene & Masek, 2012). Further studies have
302 elucidated that aversive taste memories are dependent on mushroom body neurons that form
303 the gamma and alpha lobes, the PPL1 cluster of dopamine neurons, and alpha lobe output
304 neurons, revealing a circuit regulating taste memory that differs from that controlling appetitive
305 olfactory memory (Kirkhart & Scott, 2015; P Masek, Worden, Aso, Rubin, & Keene, 2015). It will
306 be interesting to determine whether shared components regulate conditioning to fatty acids, or
307 whether distinct mushroom body circuits regulate sweet taste and fatty acid conditioning.
308 Further, examination of the central brain circuits that regulate aversive taste conditioning to
309 different classes of fatty acids will provide insight into how taste discrimination is processed
310 within the brain.

311

312 **Materials and Methods**

313 ***Drosophila* stocks and maintenance**

314 Flies were grown and maintained on standard food media (Bloomington Recipe, Genesee
315 Scientific, San Diego, CA). Flies were housed in incubators (Powers Scientific, Warminster, PA,
316 USA) on a 12:12 LD cycle at 25°C with humidity of 55-65%. The following fly strains were
317 ordered from the Bloomington Stock Center: *w*¹¹¹⁸ (#5905; (Levis, Hazelrigg, & Rubin, 1985));
318 *IR56D-GAL4* (#60708; (Koh et al., 2014)), UAS-impTNT (#28840; (Sweeney et al., 1995)), UAS-
319 TNT (#28838; (Sweeney et al., 1995)), UAS-GFP (#32186; (Pfeiffer et al., 2010)); UAS-
320 GCaMP5 (#42037; (Akerboom et al., 2012)). UAS-*Ir56d* was generated using *Ir56d* cDNA,
321 amplified with primers that generated a NotI-KpnI fragment that was cloned in the pUAS vector.
322 The *IR56d*^{GAL4} line was generated by WellGenetics (Taipei City, Taiwan) using the
323 CRISPR/Cas9 system to induce homology-dependent repair. At the gRNA target site, a dsDNA
324 donor plasmid was inserted containing a GAL4::VP16 and RFP cassette. This line was

325 generated in the w^{1118} genetic background and was validated by PCR and sequencing. All lines
326 were backcrossed to the w^{1118} fly strain. For all experiments, mated female flies aged 7-to-9
327 days were used. For ablation experiments, the antenna and/or maxillary palp were removed two
328 days post-eclosion.

329

330 **Reagents**

331 The following fatty acids were obtained from Sigma Aldrich (St Louis, MO, USA): butyric acid
332 (4C; #B103500), valeric acid (5C; #240370), hexanoic acid (6C; #21530), heptanoic acid (7C;
333 #75190), octanoic acid (8C; #O3907), nonanoic acid (9C; #N5502), and decanoic acid (10C;
334 #C1875). All fatty acids were tested at a concentration of 1% and were dissolved in water.
335 Quinine hydrochloride was also obtained from Sigma Aldrich (#Q1125), while sucrose was
336 purchased from Fisher Scientific (#FS S5-500; Hampton, New Hampshire, USA).

337

338 **Immunohistochemistry**

339 Brains were prepared as previously described (Kubrak, Lushchak, Zandawala, & Nässel, 2016).
340 Briefly, brains of 7-9 day-old female flies were dissected in ice-cold PBS and fixed in 4%
341 formaldehyde, PBS, and 0.5% Triton-X for 30 minutes at room temperature. Brains were rinsed
342 3X with PBS and 0.5% Triton-X (PBST) for 10 minutes at room temperature and then incubated
343 overnight at 4°C. The next day, brains were incubated in primary antibody (1:20 mouse nc82;
344 Iowa Hybridoma Bank; The Developmental Studies Hybridoma Bank, Iowa City, Iowa, USA)
345 diluted in 0.5% PBST at 4°C for 48 hrs. Next, the brains were rinsed 3X in 0.5% PBST 3X 10
346 minutes at room temperature and placed in secondary antibody (1:400 donkey anti-mouse
347 Alexa Fluor 647; #A-31571; ThermoFisher Scientific, Waltham, Massachusetts, USA) for 90
348 minutes at room temperature. The brains were again rinsed 3X in PBST for 10 min at room
349 temperature and then mounted in Vectashield (VECTOR Laboratories, Burlingame, CA). Brains
350 were imaged in 2µm sections on a Nikon A1R confocal microscope (Nikon, Tokyo, Japan) using

351 a 20X oil immersion objective. Images presented as the Z-stack projection through the entire
352 brain and processes using ImageJ2 (Tauber et al., 2017).

353

354 **Proboscis Extension Response**

355 Female flies were starved for 48 h prior to each experiment and then PER was measured as
356 previously described (Pavel Masek & Keene, 2013; Tauber et al., 2017). Briefly, flies were
357 anesthetized on CO₂ and then restrained inside of a cut 200 µL pipette tip (#02-404-423; Fisher
358 Scientific) so that their head and proboscis were exposed while their body and tarsi remain
359 restrained. After a 60 min acclimation period in a humidified box, flies were presented with water
360 and allowed to drink freely until satiated. Flies that did not stop responding to water within 5
361 minutes were discarded. A wick made of Kimwipe (#06-666; Fisher Scientific) was placed
362 partially inside a capillary tube (#1B120F-4; World Precision Instruments; Sarasota, FL) and
363 then saturated with tastant. The saturated wick was then manually applied to the tip of the
364 proboscis for 1-2s and proboscis extension reflex was monitored. Only full extensions were
365 counted as a positive response. Each tastant was presented a total of three times, with 1 min
366 between each presentation. PER was calculated as the percentage of proboscis extensions
367 divided by the total number of tastant presentations. For example, a fly that extends its
368 proboscis twice out of the three presentation will have a PER response of 66%.

369

370 ***In vivo* calcium imaging**

371 Female flies were starved for 48 h prior to imaging, as described (Tauber et al., 2017). Flies
372 were anaesthetized on ice and then then restrained inside of a cut 200 µL pipette tip so that
373 their head and proboscis were accessible, while their body and tarsi remain restrained. The
374 proboscis was manually extended and then a small amount of dental glue (#595953WW; Ivoclar
375 Vivadent Inc.; Amherst, NY) was applied between the labium and the side of the pipette tip,
376 ensuring the same position throughout the experiment. Next, both antennae were removed. A

377 small hole was cut into a 1 cm² piece of aluminum foil and then fixed to the fly using dental glue,
378 creating a sealed window of cuticle exposed. Artificial hemolymph (140 mM NaCl, 2mM KCl, 4.5
379 mM MgCl₂, 1.5mM CaCl₂, and 5mM HEPES-NaOH with pH = 7.1) was applied to the window
380 and then the cuticle and connective tissue were dissected to expose the SEZ. Mounted flies
381 were placed on a Nikon A1R confocal microscope and then imaged using a 20X water-dipping
382 objective lens. The pinhole was opened to allow a thicker optical section to be monitored. All
383 recordings were taken at 4Hz with 256 resolution. Similar to PER, tastants were applied to the
384 proboscis for 1-2s with a wick, which was operated using a micromanipulator (Narishige
385 International USA, Inc.; Amityville, NY). For analysis, regions of interest were drawn manually
386 around posterior IR56D projections. Baseline fluorescence was calculated as the average
387 fluorescence of the first 5 frames, beginning 10 sec prior to tastant application. For each frame,
388 the % change in fluorescence ($\% \Delta F/F$) was calculated as: (peak fluorescence - baseline
389 fluorescence)/baseline fluorescence * 100. Average fluorescence traces were created by taking
390 the average and standard error of $\% \Delta F/F$ for each recording of a specific tastant.

391

392 **Aversive Taste Memory**

393 Taste discrimination was assessed by measuring aversive taste memory, as described
394 previously (Tauber et al., 2017). Female flies were starved for 48 h prior to each experiment.
395 Flies were then anaesthetized on CO₂ and the thorax of each fly was glued to a microscope
396 slide using clear nail polish (#451D; Wet n Wild, Los Angeles, CA). Flies were acclimated to
397 these conditions in a humidified box for 60 min. For each experiment, the microscope slide was
398 mounted vertically under a dissecting microscope (#SM-1BSZ-144S; AmScope; Irvine,
399 California). Flies were water satiated prior to each experiment and in between each test/training
400 session. For tastant presentation, we used a 200 μ L pipet tip attached to a 3ml syringe (#14-
401 955-457; Fisher Scientific). For the pretest, 1% fatty acid was presented to the proboscis 3
402 times, with 1 min in between each presentation, and the number of full proboscis extensions

403 was recorded. During training, a similar protocol was used except that each tastant presentation
404 was immediately followed by 50mM quinine presentation which flies were allowed to drink it for
405 up to 2 sec or until an extended proboscis was retracted. A total of 3 training sessions were
406 performed. In between each session, the proboscis was washed with water and flies were
407 allowed to drink to satiation. To assess taste discrimination, flies were tested either with that
408 same tastant without quinine or with an untrained tastant. Another group of flies were tested as
409 described above but quinine was never presented (naïve). At the end of each experiment, flies
410 were given 1M sucrose to check for retained ability to extend proboscis and all non-responders
411 were excluded.

412

413 **Statistical Analysis**

414 All measurements are presented as bar graphs showing mean \pm standard error. Measurements
415 of PER and aversive taste memory were not normally distributed and so the non-parametric
416 Kruskal-Wallis test was used to compare two or more genotypes. To compare two or more
417 genotypes and two treatments, a restricted maximum likelihood (REML) estimation was used.
418 For data that was normally distributed (calcium imaging data), a one-way or two-way analysis of
419 variance (ANOVA) was used for comparisons between two or more genotypes and one
420 treatment or two or more genotypes and multiple treatments, respectively. All post hoc analyses
421 were performed using Sidak's multiple comparisons test. Statistical analyses and data
422 presentation were performed using InStat software (GraphPad Software 8.0; San Diego, CA).

423

424 **Acknowledgments**

425 We would like to thank members of the Keene and Dahanukar labs for technical assistance and
426 helpful discussion. This work was supported by NIH grants R01 NS085252 to ACK and
427 R01DC017390 to ACK and AD, as well as support from FAU's Jupiter Life Science Initiative.

428 **References**

- 429 Ahn, J. E., Chen, Y., & Amrein, H. (2017). Molecular basis of fatty acid taste in *Drosophila*.
430 *ELife*, 6, 1–21. <https://doi.org/10.7554/eLife.30115.001>
- 431 Akerboom, J., Chen, T.-W., Wardill, T. J., Tian, L., Marvin, J. S., Mutlu, S., ... Looger, L. L.
432 (2012). Optimization of a GCaMP Calcium Indicator for Neural Activity Imaging. *The*
433 *Journal of Neuroscience*, 32(40), 13819–13840. [https://doi.org/10.1523/JNEUROSCI.2601-](https://doi.org/10.1523/JNEUROSCI.2601-12.2012)
434 12.2012
- 435 Amin, H., & Lin, A. C. (2019). Neuronal mechanisms underlying innate and learned olfactory
436 processing in *Drosophila*. *Current Opinion in Insect Science*.
437 <https://doi.org/10.1016/j.cois.2019.06.003>
- 438 Benton, R., Vannice, K. S., Gomez-Diaz, C., & Vosshall, L. B. (2009). Variant Ionotropic
439 Glutamate Receptors as Chemosensory Receptors in *Drosophila*. *Cell*, 136(1), 149–162.
440 <https://doi.org/10.1016/j.cell.2008.12.001>
- 441 Cameron, P., Hiroi, M., Ngai, J., & Scott, K. (2010). The molecular basis for water taste in
442 *Drosophila*. *Nature*, 465(7294), 91–95. <https://doi.org/10.1038/nature09011>
- 443 Carleton, A., Accolla, R., & Simon, S. A. (2010). Coding in the mammalian gustatory system.
444 *Trends in Neurosciences*. <https://doi.org/10.1016/j.tins.2010.04.002>
- 445 Chaudhari, N., & Roper, S. D. (2010). The cell biology of taste. *Journal of Cell Biology*, 190(3),
446 285–296. <https://doi.org/10.1083/jcb.201003144>
- 447 Chen, Y.-C. D., & Dahanukar, A. (2020). Recent advances in the genetic basis of taste
448 detection in *Drosophila*. *Cellular and Molecular Life Sciences*, 77(6), 1087–1101.
449 <https://doi.org/10.1007/s00018-019-03320-0>
- 450 Chu, B., Chui, V., Mann, K., & Gordon, M. D. (2014). Presynaptic gain control drives sweet and
451 bitter taste integration in *Drosophila*. *Current Biology*, 24(17), 1978–1984.
452 <https://doi.org/10.1016/j.cub.2014.07.020>
- 453 Clyne, P. J., Warr, C. G., & Carlson, J. R. (2000). Candidate taste receptors in *Drosophila*.

- 454 *Science (New York, N.Y.)*, 287(5459), 1830–1834.
455 <https://doi.org/10.1126/science.287.5459.1830>
- 456 Cognigni, P., Felsenberg, J., & Waddell, S. (2018). Do the right thing: neural network
457 mechanisms of memory formation, expression and update in *Drosophila*. *Current Opinion*
458 *in Neurobiology*, 49, 51–58. <https://doi.org/10.1016/j.conb.2017.12.002>
- 459 Dahanukar, A., Lei, Y.-T., Kwon, J. Y., & Carlson, J. R. (2007). Two Gr Genes Underlie Sugar
460 Reception in *Drosophila*. *Neuron*, 56(3), 503–516.
461 <https://doi.org/https://doi.org/10.1016/j.neuron.2007.10.024>
- 462 DasGupta, S., & Waddell, S. (2008). Learned Odor Discrimination in *Drosophila* without
463 Combinatorial Odor Maps in the Antennal Lobe. *Current Biology*, 18(21), 1668–1674.
464 <https://doi.org/10.1016/j.cub.2008.08.071>
- 465 Devineni, A. V., Sun, B., Zhukovskaya, A., & Axel, R. (2019). Acetic acid activates distinct taste
466 pathways in *Drosophila* to elicit opposing, state-dependent feeding responses. *ELife*, 8,
467 e47677. <https://doi.org/10.7554/eLife.47677.001>
- 468 Flood, T. F., Iguchi, S., Gorczyca, M., White, B., Ito, K., & Yoshihara, M. (2013). A single pair of
469 interneurons commands the *Drosophila* feeding motor program. *Nature*, 499(7456), 83–87.
470 <https://doi.org/10.1038/nature12208>
- 471 Freeman, E. G., & Dahanukar, A. (2015). Molecular neurobiology of *Drosophila* taste. *Current*
472 *Opinion in Neurobiology*, 34, 140–148. <https://doi.org/10.1016/j.conb.2015.06.001>
- 473 Guven-Ozkan, T., & Davis, R. L. (2014). Functional neuroanatomy of *Drosophila* olfactory
474 memory formation. *Learning & Memory (Cold Spring Harbor, N.Y.)*, 21(10), 519–526.
475 <https://doi.org/10.1101/lm.034363.114>
- 476 Hallem, E. A., & Carlson, J. R. (2006). Coding of Odors by a Receptor Repertoire. *Cell*, 125(1),
477 143–160. <https://doi.org/10.1016/j.cell.2006.01.050>
- 478 Hallem, E. A., Dahanukar, A., & Carlson, J. R. (2006). Insect odor and taste receptors. *Annual*
479 *Review of Entomology*, 51(10), 113–135.

- 480 <https://doi.org/10.1146/annurev.ento.51.051705.113646>
- 481 Harris, D. T., Kallman, B. R., Mullaney, B. C., & Scott, K. (2015). Representations of Taste
482 Modality in the *Drosophila* Brain. *Neuron*, 86(6), 1449–1460.
483 <https://doi.org/10.1016/j.neuron.2015.05.026>
- 484 Inagaki, H. K., Panse, K. M., & Anderson, D. J. (2014). Independent, reciprocal
485 neuromodulatory control of sweet and bitter taste sensitivity during starvation in *Drosophila*.
486 *Neuron*, 84(4), 806–820. <https://doi.org/10.1016/j.neuron.2014.09.032>
- 487 Jiao, Y., Moon, S. J., Wang, X., Ren, Q., & Montell, C. (2008). Gr64f Is Required in Combination
488 with Other Gustatory Receptors for Sugar Detection in *Drosophila*. *Current Biology*, 18(22),
489 1797–1801. <https://doi.org/https://doi.org/10.1016/j.cub.2008.10.009>
- 490 Kang, K., Pulver, S. R., Panzano, V. C., Chang, E. C., Griffith, L. C., Theobald, D. L., & Garrity,
491 P. A. (2010). Analysis of *Drosophila* TRPA1 reveals an ancient origin for human chemical
492 nociception. *Nature*, 464(7288), 597–600. <https://doi.org/10.1038/nature08848>
- 493 Keene, A. C., & Masek, P. (2012). Optogenetic induction of aversive taste memory.
494 *Neuroscience*, 222. <https://doi.org/10.1016/j.neuroscience.2012.07.028>
- 495 Keller, A., Gerkin, R. C., Guan, Y., Dhurandhar, A., Turu, G., Szalai, B., ... Zupan, B. (2017).
496 Predicting human olfactory perception from chemical features of odor molecules. *Science*,
497 355(6327), 820–826. <https://doi.org/10.1126/science.aal2014>
- 498 Kirkhart, C., & Scott, K. (2015). Gustatory learning and processing in the *Drosophila*. *Journal of*
499 *Neuroscience*, 15(35), 5950–5958.
- 500 Koh, T. W., He, Z., Gorur-Shandilya, S., Menuz, K., Larter, N. K., Stewart, S., & Carlson, J. R.
501 (2014). The *Drosophila* IR20a Clade of Ionotropic Receptors Are Candidate Taste and
502 Pheromone Receptors. *Neuron*, 83(4), 850–865.
503 <https://doi.org/10.1016/j.neuron.2014.07.012>
- 504 Kubrak, O. I., Lushchak, O. V., Zandawala, M., & Nässel, D. R. (2016). Systemic corazonin
505 signalling modulates stress responses and metabolism in *Drosophila*. *Open Biology*, 6(11),

- 506 160152. <https://doi.org/10.1098/rsob.160152>
- 507 LeDue, E. E., Mann, K., Koch, E., Chu, B., Dakin, R., & Gordon, M. D. (2016). Starvation-
508 Induced Depotential of Bitter Taste in *Drosophila*. *Current Biology*, 26(21), 2854–2861.
509 <https://doi.org/10.1016/j.cub.2016.08.028>
- 510 Levis, R., Hazelrigg, T., & Rubin, G. M. (1985). Effects of genomic position on the expression of
511 transduced copies of the white gene of *Drosophila*. *Science (New York, N.Y.)*, 229(4713),
512 558–561. <https://doi.org/10.1126/science.2992080>
- 513 Mann, K., Gordon, M., & Scott, K. (2013). A pair of interneurons influences the choice between
514 feeding and locomotion in *Drosophila*. *Neuron*, 79(4), 754–765.
515 <https://doi.org/10.1016/j.neuron.2013.06.018>
- 516 Marella, S., Fischler, W., Kong, P., Asgarian, S., Rueckert, E., & Scott, K. (2006). Imaging taste
517 responses in the fly brain reveals a functional map of taste category and behavior. *Neuron*,
518 49(2), 285–295. <https://doi.org/10.1016/j.neuron.2005.11.037>
- 519 Marella, S., Mann, K., & Scott, K. (2012). Dopaminergic Modulation of Sucrose Acceptance
520 Behavior in *Drosophila*. *Neuron*, 73(5), 941–950.
521 <https://doi.org/10.1016/j.neuron.2011.12.032>
- 522 Masek, P., Worden, K., Aso, Y., Rubin, G., & Keene, A. (2015). A dopamine-modulated neural
523 circuit regulating aversive taste memory in *Drosophila*. *Curr. Biol.*, 25(11), 1535–1541.
- 524 Masek, Pavel, & Keene, A. C. (2013). *Drosophila* Fatty Acid Taste Signals through the PLC
525 Pathway in Sugar-Sensing Neurons. *PLoS Genetics*, 9(9).
526 <https://doi.org/10.1371/journal.pgen.1003710>
- 527 Masek, Pavel, & Scott, K. (2010). Limited taste discrimination in *Drosophila*. *Proceedings of the*
528 *National Academy of Sciences of the United States of America*, 107(33), 14833–14838.
529 <https://doi.org/10.1073/pnas.1009318107>
- 530 Masek, Pavel, Worden, K., Aso, Y., Rubin, G. M., & Keene, A. C. (2015). A dopamine-
531 modulated neural circuit regulating aversive taste memory in *drosophila*. *Current Biology*,

- 532 25(11), 1535–1541. <https://doi.org/10.1016/j.cub.2015.04.027>
- 533 Mishra, D., Thorne, N., Miyamoto, C., Jagge, C., & Amrein, H. (2018). The taste of
534 ribonucleosides: Novel macronutrients essential for larval growth are sensed by *Drosophila*
535 gustatory receptor proteins. *PLoS Biology*, 16(8), 1–19.
536 <https://doi.org/10.1371/journal.pbio.2005570>
- 537 Nara, K., Saraiva, L. R., Ye, X., & Buck, L. B. (2011). A large-scale analysis of odor coding in
538 the olfactory epithelium. *Journal of Neuroscience*, 31(25), 9179–9191.
539 <https://doi.org/10.1523/JNEUROSCI.1282-11.2011>
- 540 Parnas, M., Lin, A. C., Huetteroth, W., & Miesenb??ck, G. (2013). Odor Discrimination in
541 *Drosophila*: From Neural Population Codes to Behavior. *Neuron*, 79(5), 932–944.
542 <https://doi.org/10.1016/j.neuron.2013.08.006>
- 543 Pfeiffer, B. D., Ngo, T. T. B., Hibbard, K. L., Murphy, C., Jenett, A., Truman, J. W., & Rubin, G.
544 M. (2010). Refinement of tools for targeted gene expression in *Drosophila*. *Genetics*,
545 186(2), 735–755. <https://doi.org/10.1534/genetics.110.119917>
- 546 Pool, A. H., Kvello, P., Mann, K., Cheung, S. K., Gordon, M. D., Wang, L., & Scott, K. (2014).
547 Four GABAergic interneurons impose feeding restraint in *Drosophila*. *Neuron*, 83(1), 164–
548 177. <https://doi.org/10.1016/j.neuron.2014.05.006>
- 549 Root, C. M., Masuyama, K., Green, D. S., Enell, L. E., Nässel, D. R., Lee, C. H., & Wang, J. W.
550 (2008). A Presynaptic Gain Control Mechanism Fine-Tunes Olfactory Behavior. *Neuron*,
551 59(2), 311–321. <https://doi.org/10.1016/j.neuron.2008.07.003>
- 552 Rytz, R., Croset, V., & Benton, R. (2013). Ionotropic Receptors (IRs): Chemosensory ionotropic
553 glutamate receptors in *Drosophila* and beyond. *Insect Biochemistry and Molecular Biology*.
554 <https://doi.org/10.1016/j.ibmb.2013.02.007>
- 555 Sánchez-Alcañiz, J. A., Silbering, A. F., Croset, V., Zappia, G., Sivasubramaniam, A. K., Abuin,
556 L., ... Benton, R. (2018). An expression atlas of variant ionotropic glutamate receptors
557 identifies a molecular basis of carbonation sensing. *Nature Communications*, 9(1), 4252.

- 558 <https://doi.org/10.1038/s41467-018-06453-1>
- 559 Scott, K. (2018). Gustatory Processing in *Drosophila melanogaster*. *Annual Review of*
560 *Entomology*, 63(1), 15–30. <https://doi.org/10.1146/annurev-ento-020117-043331>
- 561 Scott, K., Brady, R., Cravchik, A., Morozov, P., Rzhetsky, A., Zuker, C., & Axel, R. (2001). A
562 Chemosensory Gene Family Encoding Candidate Gustatory and Olfactory Receptors in
563 *Drosophila*. *Cell*, 104(5), 661–673. [https://doi.org/10.1016/S0092-8674\(01\)00263-X](https://doi.org/10.1016/S0092-8674(01)00263-X)
- 564 Slone, J., Daniels, J., & Amrein, H. (2007). Sugar Receptors in *Drosophila*. *Current Biology*,
565 17(20), 1809–1816. <https://doi.org/https://doi.org/10.1016/j.cub.2007.09.027>
- 566 Sweeney, S. T., Broadie, K., Keane, J., Niemann, H., & Kane, C. J. O. (1995). Targeted
567 Expression of Tetanus Toxin Light Chain in *Drosophila* Specifically Eliminates Synaptic
568 Transmission and Causes Behavioral Defects, 14, 341–351.
- 569 Tauber, J. M., Brown, E. B., Li, Y., Yurgel, M. E., Masek, P., & Keene, A. C. (2017). A subset of
570 sweet-sensing neurons identified by IR56d are necessary and sufficient for fatty acid taste.
571 *PLOS Genetics*, 13(11), e1007059. <https://doi.org/10.1371/journal.pgen.1007059>
- 572 Thakur, D., Kim, Y., Poudel, S., Montell, C., & Lee, Y. (2017). Calcium Taste Avoidance in
573 *Drosophila*. *Neuron*, 97(1), 67-74.e4. <https://doi.org/10.1016/j.neuron.2017.11.038>
- 574 Thorne, N., Chromey, C., Bray, S., & Amrein, H. (2004). Taste Perception and Coding in
575 *Drosophila*. *Current Biology*, 14(12), 1065–1079. <https://doi.org/10.1016/j.cub.2004.05.019>
- 576 van Giesen, L., & Garrity, P. A. (2017). More than meets the IR: the expanding roles of variant
577 Ionotropic Glutamate Receptors in sensing odor, taste, temperature and moisture.
578 *F1000Research*, 6(0), 1753. <https://doi.org/10.12688/f1000research.12013.1>
- 579 Vosshall, L. B., & Stocker, R. F. (2007). Molecular architecture of smell and taste in *Drosophila*.
580 *Annual Review of Neuroscience*, 30, 505–533.
581 <https://doi.org/10.1146/annurev.neuro.30.051606.094306>
- 582 Wang, Z., Singhvi, A., Kong, P., & Scott, K. (2004). Taste Representations in the *Drosophila*
583 Brain. *Cell*, 117(7), 981–991. <https://doi.org/10.1016/j.cell.2004.06.011>

- 584 Wisotsky, Z., Medina, A., Freeman, E., & Dahanukar, A. (2011). Evolutionary differences in food
585 preference rely on Gr64e, a receptor for glycerol. *Nature Neuroscience*, *14*(12), 1534–
586 1541. <https://doi.org/10.1038/nn.2944>
- 587 Yapici, N., Cohn, R., Schusterreiter, C., Ruta, V., & Vosshall, L. B. (2016). A Taste Circuit that
588 Regulates Ingestion by Integrating Food and Hunger Signals. *Cell*, *165*(3), 715–729.
589 <https://doi.org/10.1016/j.cell.2016.02.061>
- 590 Yarmolinsky, D. A., Zuker, C. S., & Ryba, N. J. P. (2009). Common Sense about Taste: From
591 Mammals to Insects. *Cell*. <https://doi.org/10.1016/j.cell.2009.10.001>
- 592 Zhang, Y. V., Ni, J., & Montell, C. (2013). The Molecular Basis for Attractive Salt-Taste Coding
593 in *Drosophila*. *Science*, *340*(6138), 1334–1338. <https://doi.org/10.1126/science.1234133>
- 594 Zhang, Yifeng, Hoon, M. A., Chandrashekar, J., Mueller, K. L., Cook, B., Wu, D., ... Ryba, N. J.
595 P. (2003). Coding of sweet, bitter, and umami tastes: Different receptor cells sharing similar
596 signaling pathways. *Cell*, *112*(3), 293–301. [https://doi.org/10.1016/S0092-8674\(03\)00071-0](https://doi.org/10.1016/S0092-8674(03)00071-0)
597

598 **Figure Legends**

599 **Figure 1.** *Drosophila* can discriminate between short-, medium-, and long-chain fatty acids, but
600 not among medium-chain fatty acids. **A** An aversive taste memory assay was used to assess
601 FA taste discrimination. First, initial responses to a short-, medium-, or long-chain FA was
602 assessed (Pretest). Next, flies were trained by pairing this FA with quinine (Training). PER in
603 response to either the same or different FA was then tested in the absence of quinine (Test). In
604 control experiments (Naïve), the same procedure was followed, but quinine was not applied to
605 the proboscis. **B** The pairing of medium-chain hexanoic acid (6C) and quinine (red) results in a
606 significant reduction in PER compared to naïve flies. After training, PER response to 6C was
607 significantly lower in trained flies compared to naïve flies ($P < 0.0001$), but there was no
608 difference in PER to short-chain valeric acid (5C; $P = 0.6864$). REML: $F_{1,80} = 7.329$, $P = 0.0003$,
609 with Sidak's Test for multiple comparisons; $N = 40-42$. **C** The pairing of medium-chain hexanoic
610 acid (6C) and quinine (red) results in a significant reduction in PER compared to naïve flies.
611 After training, PER response to 6C was significantly lower in trained flies compared to naïve
612 flies ($P < 0.0001$), but there was no difference in PER to long-chain nonanoic acid (9C;
613 $P = 0.3346$). REML: $F_{1,64} = 6.296$, $P = 0.0146$, with Sidak's Test for multiple comparisons; $N = 33$. **D**
614 The pairing of short-chain valeric acid (5C) and quinine (red) results in a significant reduction in
615 PER compared to naïve flies. After training, PER response to 5C was significantly lower in
616 trained flies compared to naïve flies ($P = 0.0014$), but there was no difference in PER to long-
617 chain nonanoic acid (9C; $P = 0.0789$). REML: $F_{1,46} = 2.721$, $P = 0.0105$, with Sidak's Test for
618 multiple comparisons; $N = 24$. **E** The pairing of medium-chain hexanoic acid (6C) and quinine
619 (red) results in a significant reduction in PER compared to naïve flies. After training, PER to both
620 6C and medium-chain heptanoic acid (7C) was significantly lower in trained flies compared to
621 naïve flies (6C: $P < 0.0001$; 7C: $P < 0.0001$). REML: $F_{1,81} = 45.88$, $P < 0.0001$, with Sidak's Test for
622 multiple comparisons; $N = 41-42$. **F** The pairing of medium-chain hexanoic acid (6C) and quinine
623 (red) results in a significant reduction in PER compared to naïve flies. After training, PER to both

624 6C and medium-chain octanoic acid (8C) was significantly lower in trained flies compared to
625 naïve flies (6C: $P < 0.0001$; 8C: $P < 0.0001$). REML: $F_{1,65} = 32.76$, $P < 0.0001$, with Sidak's Test for
626 multiple comparisons; N=33-34. **G** The pairing of medium-chain heptanoic acid (7C) and quinine
627 (red) results in a significant reduction in PER compared to naïve flies. After training, PER to both
628 7C and medium-chain octanoic acid (8C) was significantly lower in trained flies compared to
629 naïve flies (7C: $P < 0.0001$; 8C: $P < 0.0001$). REML: $F_{1,72} = 33.67$, $P < 0.0001$, with Sidak's Test for
630 multiple comparisons; N=37.

631

632 **Figure 2.** Ablation of chemosensory organs has no effect on the ability of *Drosophila* to
633 discriminate between short-, medium-, and long-chain fatty acids. Aversive taste memory was
634 measured as described in Figure 4A. Flies were trained by pairing medium-chain hexanoic acid
635 (6C) with quinine (Training; See Figure S3) and then PER in response to either sucrose, short-
636 chain valeric acid (5C), or long-chain nonanoic acid (9C) was measured in the absence of
637 quinine (Test). **A** Aversive taste memory was measured in unmanipulated control flies (first
638 panel), in flies without antennae (second panel), maxillary palps (third panel), or both antennae
639 and maxillary palps (fourth panel). **B** For all ablation treatments, taste memory to medium-chain
640 hexanoic acid (6C) was significantly lower in trained flies compared to naïve flies, but there was
641 no difference in PER to sucrose. REML: $F_{1,86} = 42.41$, $P < 0.0001$, with Sidak's Test for multiple
642 comparisons; N=13-26. **C** For all ablation treatments, taste memory to 6C was significantly
643 lower in trained flies compared to naïve flies, but there was no difference in PER to short-chain
644 valeric acid (5C). REML: $F_{1,103} = 51.87$, $P < 0.0001$, with Sidak's Test for multiple comparisons;
645 N=19-31. **D** For all ablation treatments, taste memory to 6C was significantly lower in trained
646 flies compared to naïve flies, but there was no difference in PER to long-chain nonanoic acid
647 (9C). REML: $F_{1,97} = 11.47$, $P = 0.0010$, with Sidak's Test for multiple comparisons; N=22-27.

648

649 **Figure 3.** Silencing *IR56D*-expressing neurons reduces taste perception to medium chain fatty
650 acids. **A** Proboscis extension response (PER). PER was measured in female flies after 48 hrs of
651 starvation. Either sucrose or fatty acid was applied to the fly's labellum for a maximum of two
652 seconds and then removed to observe proboscis extension reflex. **B** Blocking synaptic release
653 by genetic expression of light-chain tetanus toxin (UAS-TNT) in *IR56D*-expressing neurons has
654 no effect on PER to sucrose compared to control flies expressing an inactive form of tetanus
655 toxin (UAS-impTNT). Mann Whitney Test: $U = 595$, $P=0.8410$; $N=35$. **C** Silencing *IR56D*-
656 expressing neurons significantly reduces PER to medium chain fatty acids (6C-8C), but has no
657 effect on PER to either short- (4C,5C) or long-chain fatty acids (9C,10C). REML: $F_{1,406} = 25.03$,
658 $P<0.0001$, with Sidak's Test for multiple comparisons; $N=24-45$.

659
660 **Figure 4.** *IR56D* mediates taste perception to medium-chain fatty acids. **A** *IR56d^{GAL4}* was
661 generated using the CRISPR/Cas9 system. In *IR56d^{GAL4}* flies, the *IR56D* gene was replaced by
662 GAL4 and RFP elements (red boxes). The relative location and orientation of genes in the
663 region are represented as gray arrows. **(B-E)** Expression pattern of *IR56d^{GAL4}* is visualized with
664 GFP. *IR56D*-expressing neurons are located on the **(B)** labellum and project to the **(C)**
665 subesophagael zone of the brain. Distinct regions of projection include the **(D)** posterior and **(E)**
666 anterior subesophagael zones. Background staining is NC82 antibody (magenta). Scale bar =
667 50 μ m. **F** Sucrose taste perception is similar in control and *IR56d^{GAL4}* mutant flies. Kruskal-Wallis
668 Test: $H = 0.1758$, $P=0.9814$, with Dunn's Test for multiple comparisons; $N=33-40$. **G** The
669 *IR56d^{GAL4}* flies have reduced PER to medium-chain fatty acids (6C-8C) relative to control,
670 *IR56d^{GAL4}* heterozygotes, and *IR56d^{GAL4}* rescue flies. However, all genotypes respond similarly
671 to both short- and long-chain fatty acids (4C,5C; 9C,10C). REML: $F_{3,850} = 17.80$, $P<0.0001$, with
672 Tukey Test for multiple comparisons; $N=28-40$.

673

674 **Figure 5.** Neuronal activity of *IR56d*^{GAL4} mutant flies is reduced in response to medium-chain
675 fatty acids. **A** Diagram of live-imaging experimental protocol. A tastant is applied to the
676 proboscis while fluorescence is recorded simultaneously. **(B-D)** Representative pseudocolor
677 images of calcium activity of the posterior projections of *IR56D* neurons in response to water
678 **(B)**, 10mM sucrose **(C)**, or 1% hexanoic acid **(D)**. Scale bar = 50 μ m. **(E-G)** Activity traces of the
679 posterior projections of *IR56D* neurons in response to each tastant in the **(E)** *IR56d*^{GAL4}
680 heterozygote controls, **(F)** *IR56d*^{GAL4} mutants, and **(G)** *IR56d*^{GAL4} rescue flies. The shaded
681 region of each trace indicates \pm SEM. **H** Average peak change in fluorescence for data shown in
682 E-G. Neuronal responses of to medium-chain fatty acids (6C-8C) are significantly reduced in
683 *IR56d*^{GAL4} mutants compared to *IR56d*^{GAL4} heterozygote controls and *IR56d*^{GAL4} rescue flies. All
684 genotypes respond similarly to both short- and long-chain fatty acids (4C,5C; 9C,10C), as well
685 as to water and sucrose. Two-way ANOVA: $F_{2,256} = 23.67$, $P < 0.0001$, with Sidak's Test for
686 multiple comparisons; N=8-14.

Figure 1

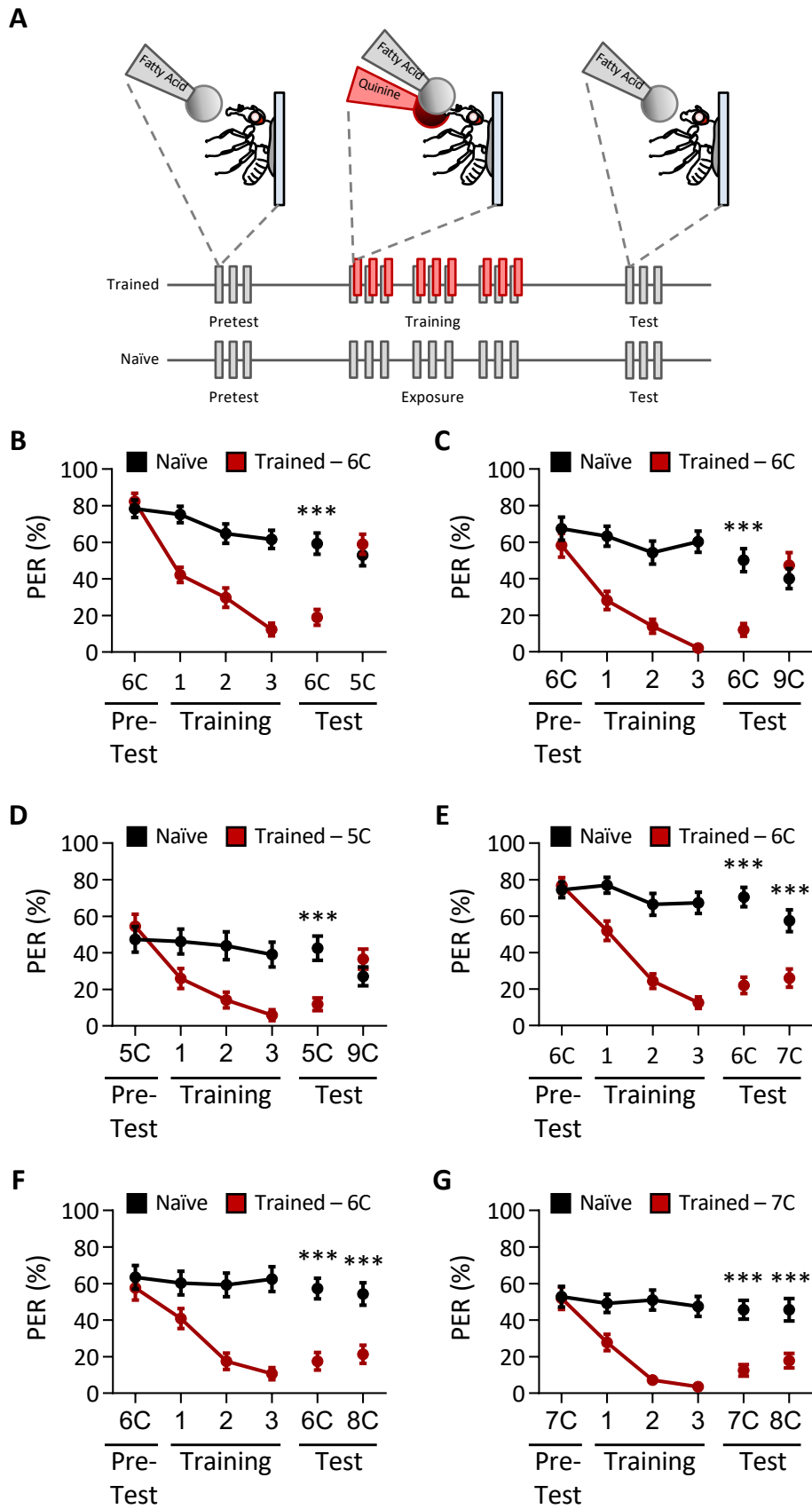


Figure 2

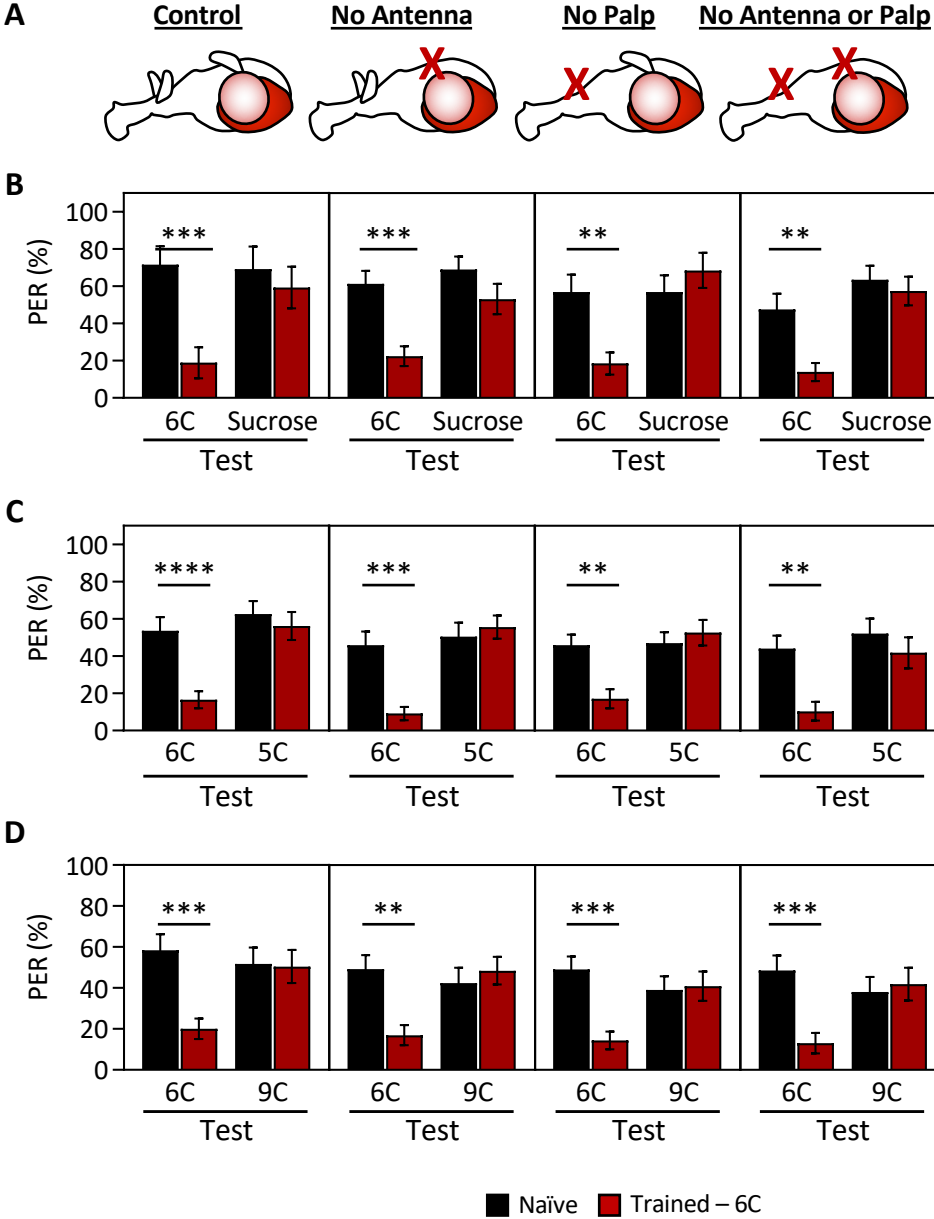
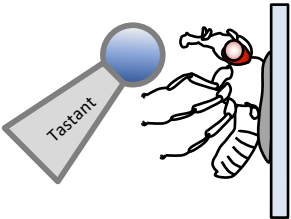
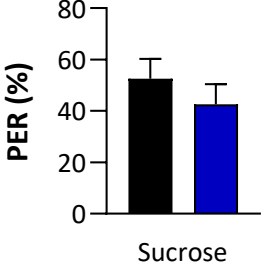


Figure 3

A



B



■ Control: *IR56D-GAL4 > UAS-impTNT*
■ Mutant: *IR56D-GAL4 > UAS-TNT*

C

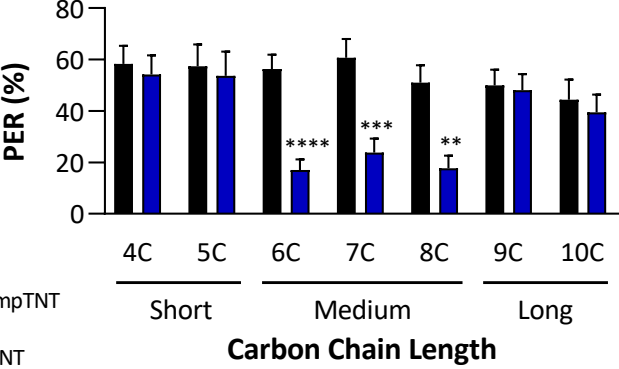
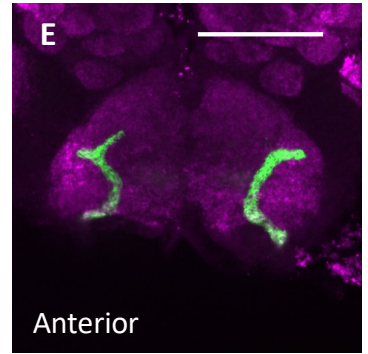
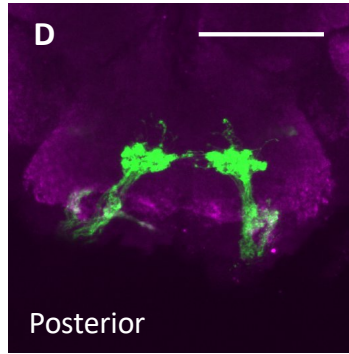
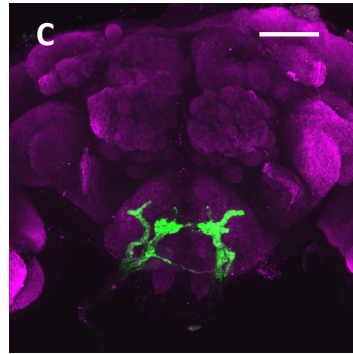
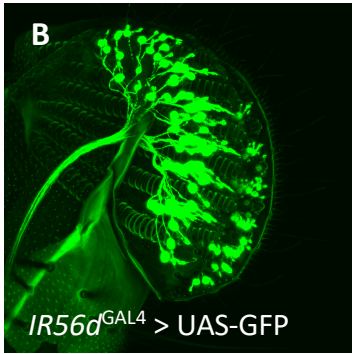
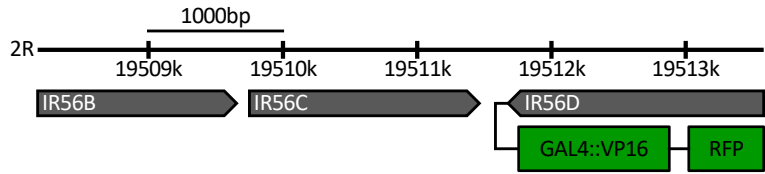
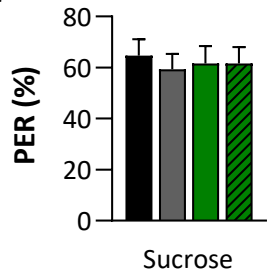


Figure 4

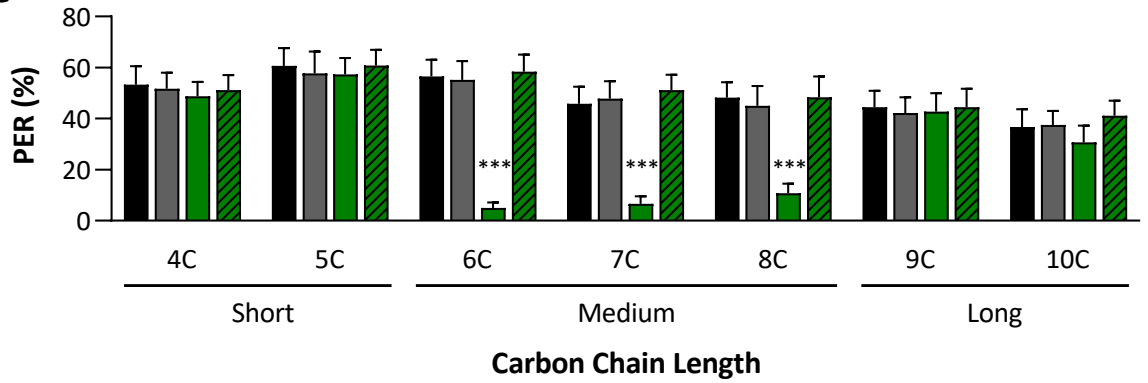
A



F



G



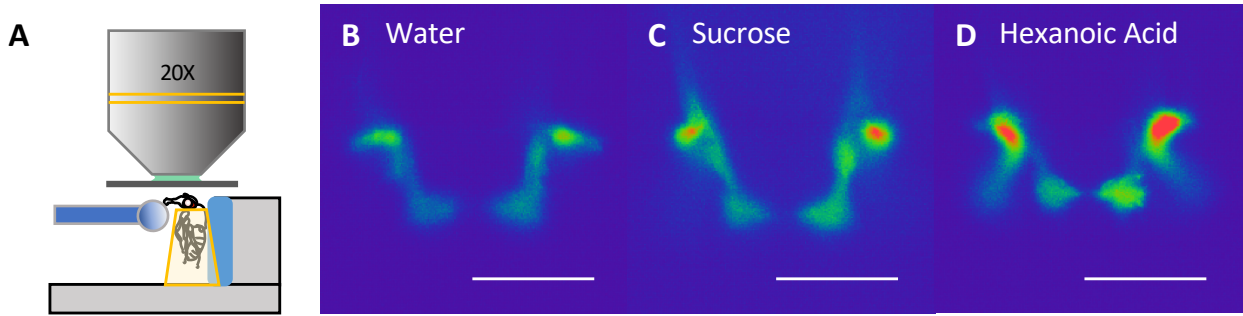
Control: +/+

Heterozygote: *IR56d^{GAL4}/+*

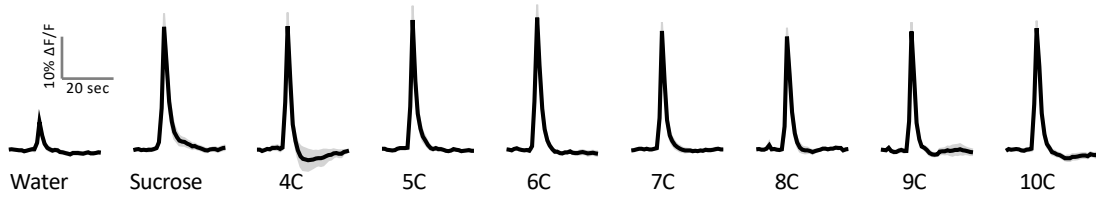
IR56D Mutant: *IR56d^{GAL4}*

Rescue: *IR56d^{GAL4}; UAS-IR56D/+*

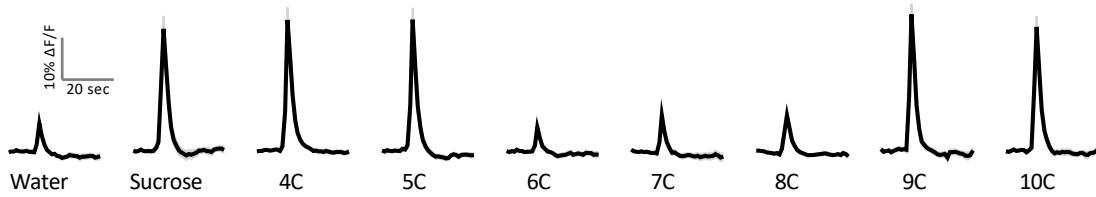
Figure 5



E Control: $\Delta IR56D/+$; UAS-GCamp6/+



F IR56DCRISPR: $\Delta IR56D$; UAS-GCamp6/+



G Rescue: $\Delta IR56D$; UAS-*IR56D*/UAS-GCamp6

